Microwave Measurement of Temperature and Current Dependences of Surface Impedance for High-T_c Superconductors

Yoshio Kobayashi, *Member, IEEE*, Tadashi Imai, and Hiroyuki Kayano

Abstract—**Perturbation formulas for TE_{011} mode dielectric rod resonator and for a TE_{011} mode circular cavity resonator are derived to determine the surface impedance $Z_s(=R_s+jX_s)$ of superconductors from measured values of resonant frequencies and unloaded Q. Also, the relation between the maximum surface current density of a superconductor, J_s (A/m), and output power from a signal generator P_O (W), is derived. On the basis of these analytical results, a measurement technique is proposed to evaluate the temperature and J_s dependences of Z_s for superconductors. The measured results of the temperature dependence of Z_s for YBCO and copper plates, which are obtained from the f_0 and Q_u values measured for the dielectric resonator and for the cavity resonator, are presented. From these results, it is verified that the dielectric resonator is suitable for measuring X_s for YBCO. Furthermore, from these Z_s values the temperature dependences of the skin depth δ and the penetration depth λ, and those of the complex conductivity $\sigma_r - j\sigma_i$ are obtained on the basis of the two-fluid model. These measured values agree well with the theoretical curves calculated by introducing the concept of the residual normal state conductivity σ_{res} into σ_r. From the J_s dependences of Z_s measured for the YBCO and copper plates, it is shown that the R_s of copper does not depend on J_s, that the value for YBCO has a strong J_s dependence, and that X_s of YBCO has little dependence on J_s. It is verified that a dielectric resonator is preferred for measuring the J_s dependence of Z_s, because of energy concentration, compared with a cavity resonator.**

I. Introduction

DESIGNING microwave devices fabricated using high-T_c superconductors requires the temperature, frequency, and surface current dependences of the surface impedance $Z_s = R_s + jX_s$, where R_s is the surface resistance and X_s is the surface reactance. A conclusion derived theoretically from the two-fluid model is that R_s is proportional to ω^2 and X_s is proportional to ω [1]. Many experimental papers have been presented recently for the frequency dependence of R_s [2]–[5] and have suggested the validity of the ω^2 dependences of R_s. On the other hand, the estimation of the surface current dependences of R_s has not been discussed so far, although the power dependences of the unloaded or loaded Q have been measured for certain resonators [6]–[8]. For X_s, furthermore, even measured results have not been presented because of experimental difficulties.

In this paper, two perturbational techniques are discussed for measuring the temperature dependences of X_s as well as R_s; one is a TE_{011} mode dielectric resonator method and the other is a TE_{011} mode cavity resonator method. The former is applicable in the frequency range of 5 to 20 GHz and the latter in the range of 15 to 100 GHz when we use a superconducting plate sample 26 mm in diameter [9]. Then a measurement technique is proposed for evaluating the surface current dependence of Z_s, after the relationship between the maximum surface current density on a superconductor and output power from a signal generator is derived [10].

The usefulness of these techniques is verified by measuring the temperature and J_s dependence of R_s and X_s for a $YBa_2Cu_3O_{7-\delta}$ bulk plate, which is abbreviated as a YBCO plate.

II. Measurement Principle

A. Perturbation Formulas for Z_s

Fig. 1(a) shows a TE_{011} mode dielectric rod resonator placed between a lower perfect-conductor plate with $Z_{sl} = R_{sl} + jX_{sl} = 0$, where the subscript l denotes the lower side, and an upper conductor plate with a finite value of Z_s, such as a superconductor or a metal plate. See Appendix I for the definition of Z_s. In this analysis, a dielectric rod having relative permittivity ϵ_r, diameter $D = 2R$, and length L is assumed to be lossless. Fig. 1(b) shows a TE_{011} mode circular cavity with diameter $D = 2R$ and length L which contains a perfect-conductor cylinder with $Z_{scy} = 0$, a lower perfect conductor plate with $Z_{sl} = 0$, and an upper conductor plate with a finite Z_s value. Fig. 1(c) shows an equivalent circuit for these resonators, from which the resonance condition is given by

$$Z_s + jZ_\beta \tan \beta L = 0, \qquad Z_\beta = \frac{\omega\mu}{\beta} \tag{1}$$

where $\mu = \mu_0 = 4\pi \times 10^{-7}$ (H/m), and Z_β and β are the characteristic impedance and the phase constant in a

Manuscript received October 23, 1990; revised April 29, 1991.

Y. Kobayashi and H. Kayano are with the Department of Electrical Engineering, Saitama University, Shimo-Okubo 255, Urawa, Saitama 338, Japan.

T. Imai was with the Department of Electrical Engineering, Saitama University, Saitama, Japan. He is now with Canon Electronics Inc., Chichibu, Saitama 369-18, Japan.

IEEE Log Number 9101269.

0018-9480/91/0900-1530$01.00 ©1991 IEEE

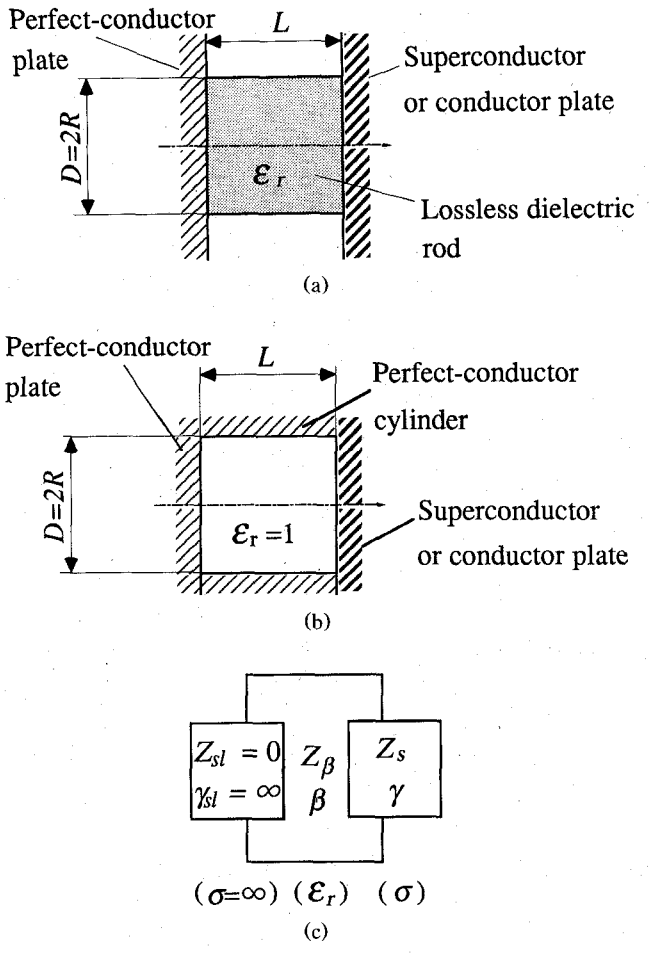

Fig. 1. Analytical model. (a) TE_{011} mode dielectric rod resonator. (b) TE_{011} mode circular cylindrical cavity. (c) Equivalent circuit.

dielectric waveguide or in a circular waveguide, respectively. We then introduce a perturbational quantity of complex angular frequency $\Delta\dot{\omega}/\omega$ into (1):

$$\frac{\Delta\dot{\omega}}{\omega} = \frac{\Delta f}{f} + j\frac{1}{2Q_s}, \qquad \Delta f = f_0 - f \tag{2}$$

where f is the resonant frequency when $Z_s = 0$, and f_0 and Q_s are the resonant frequency and Q caused by ohmic loss in the upper conductor when $Z_s \neq 0$. Furthermore, taking the first-order approximation of (1), we can derive a perturbation formula for Z_s; that is,

$$Z_s = 960\pi^2\left(\frac{L}{\lambda_0}\right)^3\frac{\epsilon_r + W}{1+W}\left(-j\frac{\Delta\dot{\omega}}{\omega}\right) \tag{3}$$

for the dielectric resonator in Fig. 1(a) (see Appendix II) and

$$Z_s = 960\pi^2\left(\frac{L}{\lambda_0}\right)^3\left(-j\frac{\Delta\dot{\omega}}{\omega}\right) \tag{4}$$

for the cavity resonator in Fig. 1(b), where $\lambda_0 = c/f_0$, c is the light velocity in vacuum, and W is given by (A23).

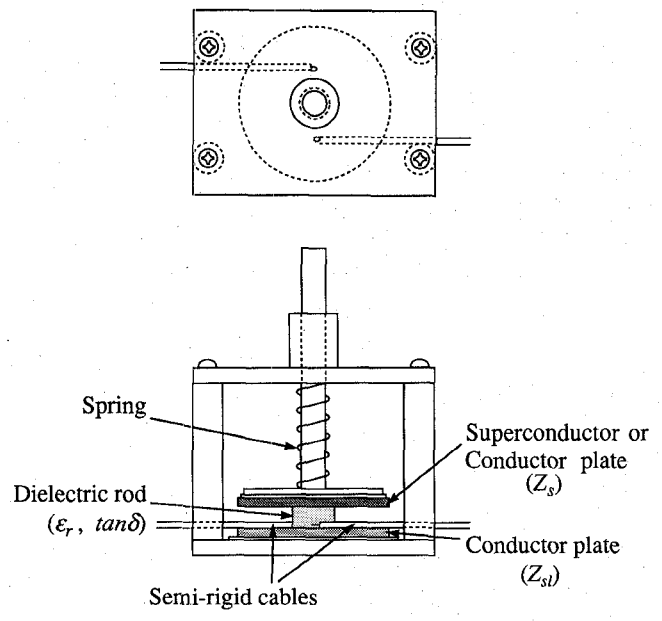

Fig. 2. A structure of TE_{011} mode dielectric rod resonator.

In particular, the relation $R_s = X_s$ holds when the upper conductor plate is in the normal state (see Appendix I); thus the resonant frequency for $Z_s = 0$ is determined from the measured values of f_0 and Q_s by

$$f = \frac{2Q_s}{2Q_s - 1}f_0 \tag{5}$$

which is derived from (2)–(4). In actual resonators, R_{sl}, R_{scy}, and the loss tangent of dielectric $\tan\delta$ are not zero. In this case, Q_s can be obtained by removing the effects caused by these losses from a measured Q_u value; that is,

$$\frac{1}{Q_s} = \frac{1}{Q_u} - \frac{R_{sl}}{480\pi^2}\left(\frac{\lambda_0}{L}\right)^3\frac{1+W}{\epsilon_r + W} - \frac{\tan\delta}{1+W/\epsilon_r} \tag{6}$$

for the dielectric resonator and

$$\frac{1}{Q_s} = \frac{1}{Q_u} - \frac{R_{sl}}{480\pi^2}\left(\frac{\lambda_0}{L}\right)^3 - \frac{u_{01}'^2 R_{scy}}{60\pi^4}\left(\frac{\lambda_0}{D}\right)^3 \tag{7}$$

for the cavity, where $u'_{01} = 3.8317$.

B. Maximum Surface Current Density J_s

Figs. 2 and 3 show structures of a TE_{01l} mode dielectric rod resonator and a TE_{01l} mode cavity resonator used for experiment, which are set in a He-gas closed-loop cryostat. These resonators are excited and detected by two semirigid cables, each having a small loop at the top. The equivalent circuit of these resonators is given in Fig. 4 if the coupling coefficient at the input port, β_c, equals that at the output port. Here β_c, the external Q (Q_e), the unloaded Q (Q_u), and the loaded Q (Q_L), as is well

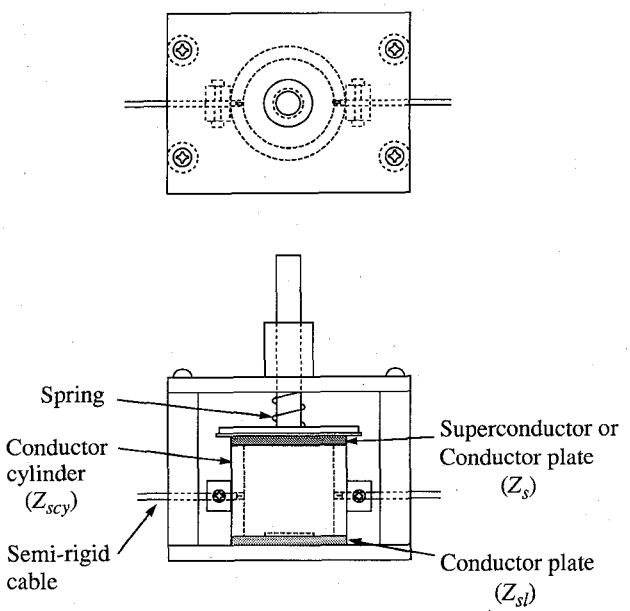

Fig. 3. A structure of TE_{011} mode cylindrical cavity resonator.

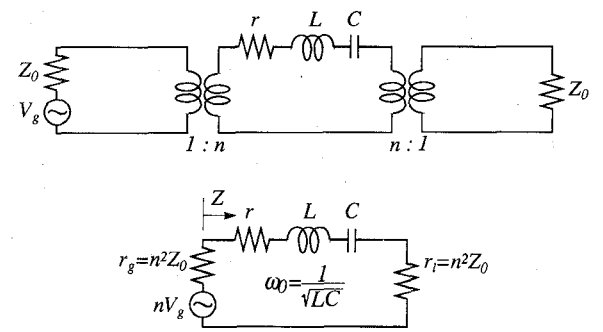

Fig. 4. Equivalent circuit of Figs. 2 and 3.

known, are given by

$$\beta_c = \frac{r_g}{r} = \frac{r_l}{r} = \frac{n^2 Z_0}{r} = \frac{Q_u}{Q_e} \tag{8}$$

$$Q_e = \frac{\omega_0 L}{r_g} = \frac{\omega_0 L}{r_l} \tag{9}$$

$$Q_u = \frac{\omega_0 L}{r} \tag{10}$$

$$Q_L = \frac{\omega_0 L}{r_g + r_l + r} = \frac{Q_u}{1+2\beta_c} \tag{11}$$

respectively. Also, from the resonance curve on a network analyzer, the Q_L and Q_u values are determined by

$$Q_L = \frac{f_0}{f_2 - f_1} \tag{12}$$

$$Q_u = \frac{Q_L}{1-a} \tag{13}$$

$$a = \frac{2\beta_c}{1+2\beta_c} = 10^{-IL(\mathrm{dB})/20} \tag{14}$$

where $f_2 - f_1$ is the half-power bandwidth, and IL is the insertion loss at f_0 in dB.

We shall derive the relationship between P_O and J_s, where P_O is output power from a signal generator in W and J_s is the maximum surface current density in A/m which flows on the upper conductor plate in the circumferential direction. Also J_s corresponds to the value at $r = 1.841R/u$ for the dielectric resonator or at $r = 1.841R/3.8317$ for the cavity resonator, where u is given by (A13). With reference to Fig. 4, the relation between the power dissipated in the resonator P_r and P_O is given by

$$P_r = \frac{4\beta_c}{(1+2\beta_c)^2} P_O = 2a(1-a)P_O. \tag{15}$$

For the dielectric resonator, furthermore, the relation between P_r and J_s is given by

$$P_r = P_d + P_u + P_l = A^2 F = J_s^2 F \tag{16}$$

where P_d is the dielectric loss, P_u is the upper conductor loss, P_l is the lower conductor loss, and A is the maximum amplitude of the radial component of the magnetic field which corresponds to J_s. Calculating P_d, P_u, and P_l from the field components for the TE_{01l} mode (see Appendix III), we obtain

$$F = \frac{\pi D^2 \left[J_1^2(u) - J_0(u) J_2(u) \right]}{8} \cdot \left[\left(\frac{L}{\lambda_0} \right)^3 \frac{480\pi^2 \epsilon_r \tan\delta}{l^2} + (1+W)(R_s + R_{sl}) \right] \tag{17}$$

where $J_n(u)$ is the Bessel function of the first kind and u is given by (A13). In a similar way we can derive F for the cavity resonator, that is,

$$F = \frac{\pi D^2 J_0^2(u'_{01})}{8} \left[\frac{8u'^2_{01}}{l^2 \pi^2} \left(\frac{L}{D} \right)^3 R_{s\,\mathrm{cy}} + R_{sl} + R_s \right]. \tag{18}$$

Using (15)–(18), we obtain the relation between J_s and P_O, that is,

$$J_s = \sqrt{\frac{2a(1-a)P_O}{F}}. \tag{19}$$

Since the conductor and dielectric losses usually decrease as the temperature is lowered, Q_u and Q_L increase and IL decreases, as is seen from (8)–(14) [10]. Hence, if we measure the temperature dependence of Z_s as keeping P_O constant, a change of J_s occurs and may influence the Z_s measurement. To avoid this effect, P_O or β_c should be adjusted to keep a small value of J_s constant during the measurement. In this experiment a method of P_O adjustment was used because of a lack of means to adjust β_c mechanically for the resonator set in the cryostat. In this case, P_{O2} at T_2 is determined from P_{O1} at T_1 by

$$P_{O2} = \frac{a_1(1-a_1)F_2}{a_2(1-a_2)F_1} P_{O1} \tag{20}$$

which is derived from (19).

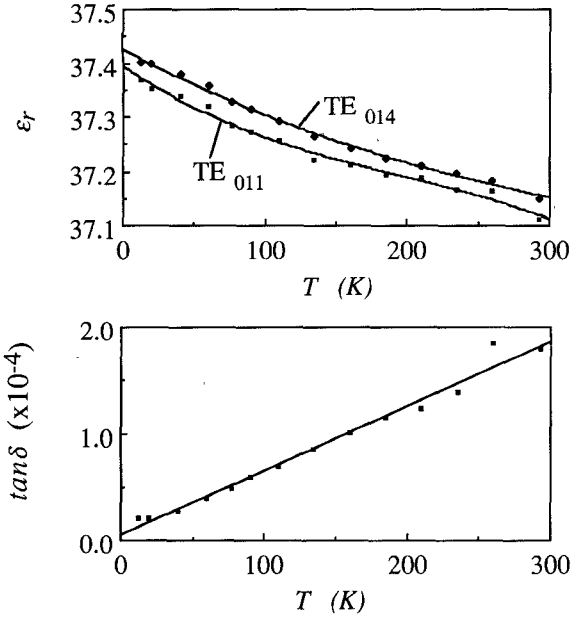

Fig. 5. Measured results of ϵ_r and $\tan\delta$ for $(ZrSn)TiO_4$ ceramic rods at 10.4 GHz.

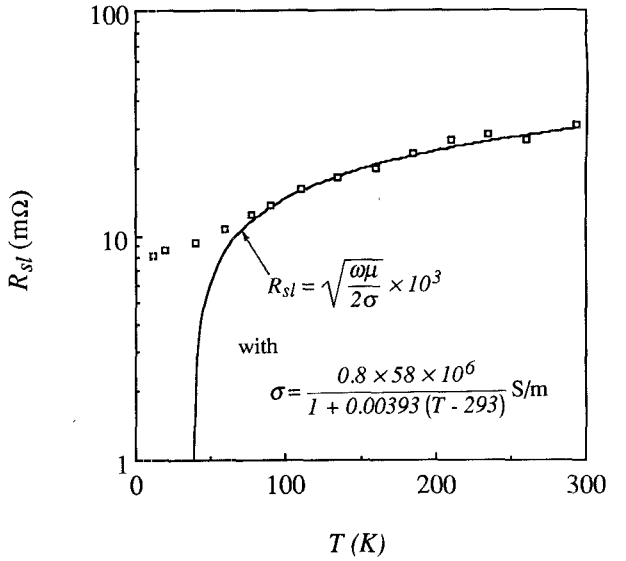

Fig. 6. Measured and calculated results of R_{sl} for copper at 10.4 GHz.

III. Measured Results

A. ϵ_r and $\tan\delta$ for $(ZrSn)TiO_4$ and R_{sl} for Copper

Before measuring the Z_s value, the temperature dependences of ϵ_r, $\tan\delta$, and R_{sl} were measured at 10.4 GHz by using TE_{011} and TE_{014} mode dielectric resonators placed between two cooper plates of diameter $d_0 =$ 30 mm. This procedure is described in [11]. These dielectric resonators consist of two $(ZrSn)TiO_4$ rods having $D = 7.30$ mm and $L = 3.07$ and 12.30 mm (Murat Mfg. Co., Ltd.). The coefficient of thermal linear expansion is assumed to be $\tau_d = 6.5$ ppm/K in the temperature range 11–300 K. Fig. 5 shows the measured results for the $(ZrSn)TiO_4$ rods. The $\tan\delta$ value increases linearly with temperature. Fig. 6 shows the measured results for the copper plates. The solid curve in Fig. 6 indicates the calculated R_{sl} values when σ is assumed to be 80% of copper conductivity. This curve is effective in the temperature range above 100 K. In addition, the accuracies of the measured values are $\pm 0.2\%$ for ϵ_r, $\pm 5\%$ for $\tan\delta$, and $\pm 5\%$ for R_{sl}.

B. Temperature Dependence of Z_s for YBCO

The upper copper plate was then replaced with a YBCO plate of $d_0 = 28$ mm in the TE_{011} mode dielectric resonator shown in Fig. 2. Fig. 7(a) shows the measured result of Q_u in this case (YBCO-Cu), together with that for two copper plates (Cu-Cu). Similarly, the measured results of f_0 are shown in Fig. 7(b) by the solid squares A and the open squares B, respectively. Curves C and D for $Z_s = 0$ were calculated on the assumption that $R_s = X_s$ from (5) to (6) using the values of ϵ_r, $\tan\delta$, R_{sl}, Q_u, and f_0 given in Figs. 5 to 7. Curve D does not have a discontinuity in the entire range of temperature, since copper is always in the normal state ($R_s = X_s$). On the other hand, curve C has a discontinuity at $T = T_c = 92$ K, where T_c is the critical temperature of the YBCO; this is because the YBCO plate is in the superconducting state ($R_s \neq X_s$) below 92 K. The difference between curves C and D near room temperature can be explained by the uncertain contacts which occur when the dielectric rod is set between two plates [9]. Assuming the same condition of the contacts to be realized, we can shift curve D into the broken line E by 9.3 MHz. Thus the Δf values necessary for calculating X_s are given by the difference between the solid squares A and the broken line E. The values of R_s and X_s can be obtained from (3) using the Q_s and Δf values described above; the skin depth, δ, and the penetration depth, λ, are from (A10); and the complex conductivity, $\sigma_r - j\sigma_i$, is from (A11). These results are indicated in, respectively, parts (a), (b), and (c) of Fig. 8 by dots. In these curves figures the theoretical values from the two-fluid model are also indicated by curves, which were calculated for the case where London's penetration depth at $T = 0$ K is $\lambda = 1.91$ μm, the normal state conductivity is $\sigma_n = 3.67 \times 10^5$ S/m, and the residual normal state conductivity is $\sigma_{res} = 1.0 \times 10^5$ S/m (see Appendix I). A detailed discussion of σ_{res} will be found in [12]. The agreement between theory and experiment is good for these data. However it is noted that there are repeatable accuracies of $\pm 20\%$ for R_s and of $\pm 100\%$ for X_s, because the sample was not flat.

A similar measurement was performed using a TE_{011} mode cavity resonator with $D = 24.63$ mm and $L = 8.11$ mm at 23.7 GHz. The Z_s results obtained using (4) are shown in Fig. 9. The amount of scatter in X_s is much larger than that for the dielectric resonator. According to calculation, for the dielectric resonator the change of resonant frequency caused by the change of the skin depth of YBCO is about 10 times more sensitive than that for the cavity resonator. This fact verifies that the dielectric resonator method is preferred for measuring X_s.

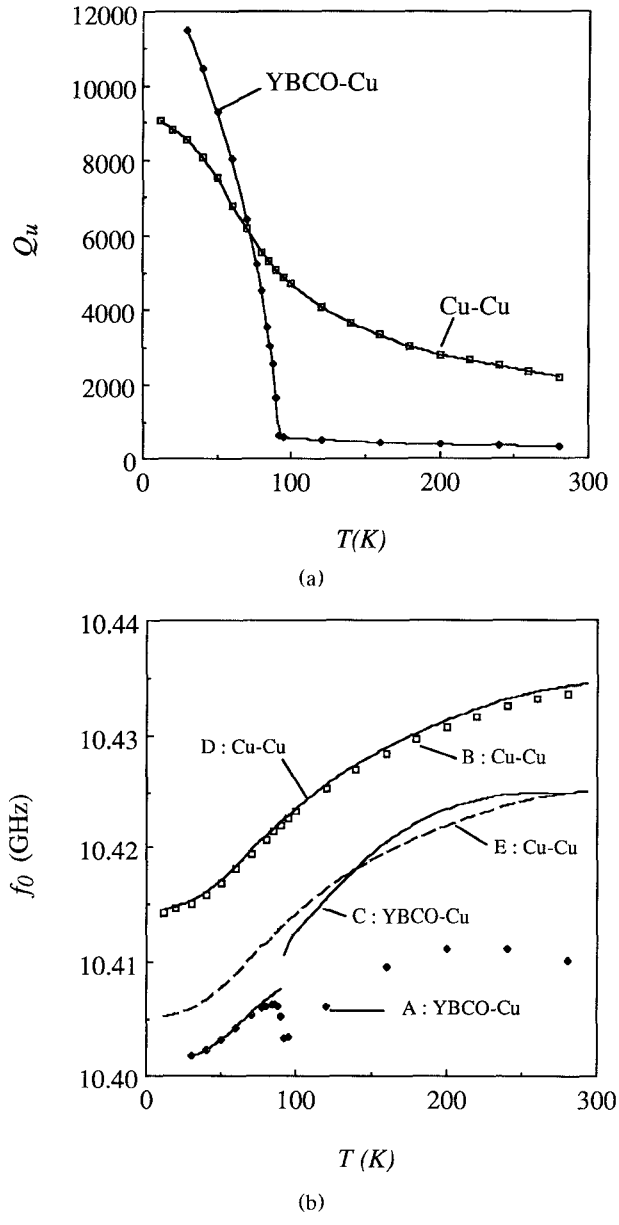

Fig. 7. Measured Q_u and f_0 results for TE_{011} dielectric rod resonators in two cases of copper-copper plates (Cu-Cu) and YBCO-copper plates (YBCO-Cu). (a) Q_u versus T. (b) f_0 versus T.

The experiment described above was performed near $P_O = 0$ dBm. But if a larger value of P_O is used during the measurement of the temperature dependence of R_s, the error may rise. To verify this, the temperature dependences of R_s and J_s for the YBCO plate were measured by using the dielectric resonator in two cases: $P_O = 16.5$ dBm constant and $J_s = 317$ A/m at $r = 0.6R$ constant. Parts (a) and (b) of Fig. 10 show the measured results. The R_s value at 11 K for $P_O = 16.5$ dBm constant is 29% higher than that for $J_s = 317$ A/m constant, because $J_s = 317$ A/m at 77 K increases to 522 A/m at 11 K, as shown in Fig. 10(b). As a result, measurements of this kind should be performed with small power from a generator. However a change of X_s was not observed in this case, because the influence of P_O on f_0 was negligible.

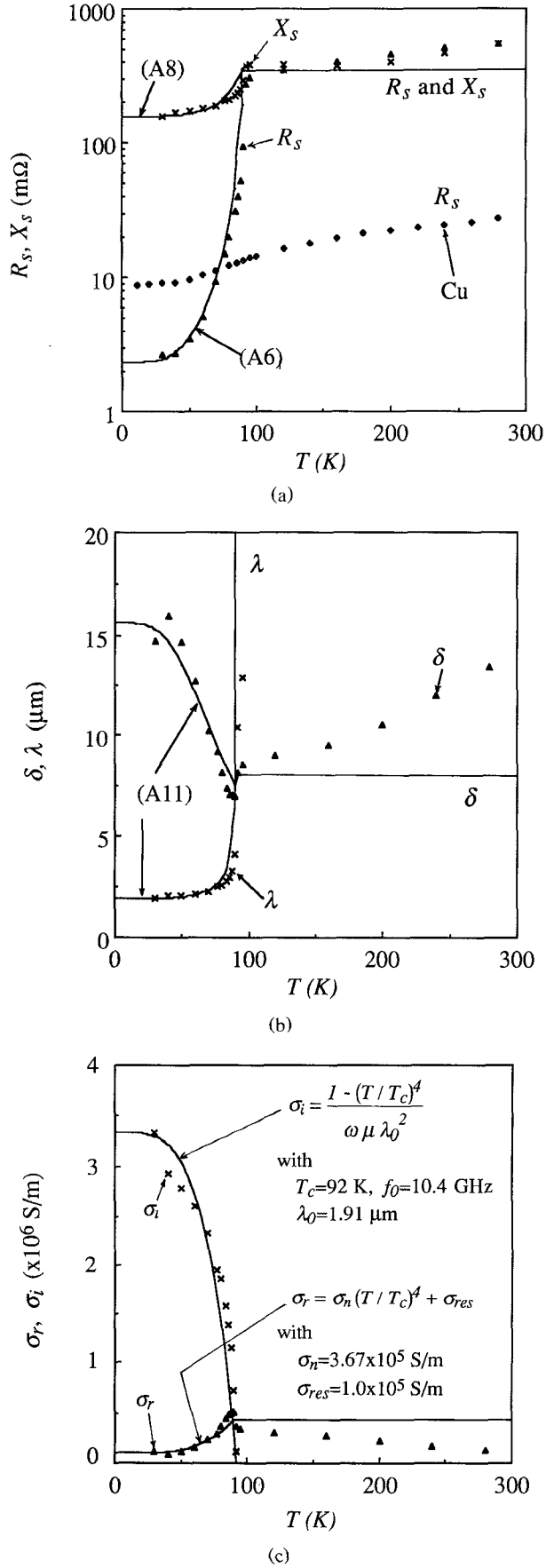

Fig. 8. Measured and calculated results for YBCO at 10.4 GHz by dielectric resonator method. (a) R_s and X_s versus T. (b) δ and λ versus T. (c) σ_r and σ_i versus T.

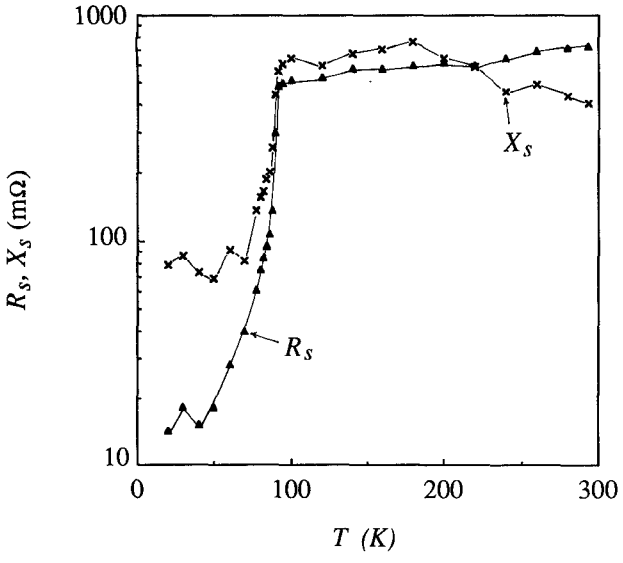

Fig. 9. Measured results of R_s and X_s for YBCO at 23.7 GHz by cavity resonator method.

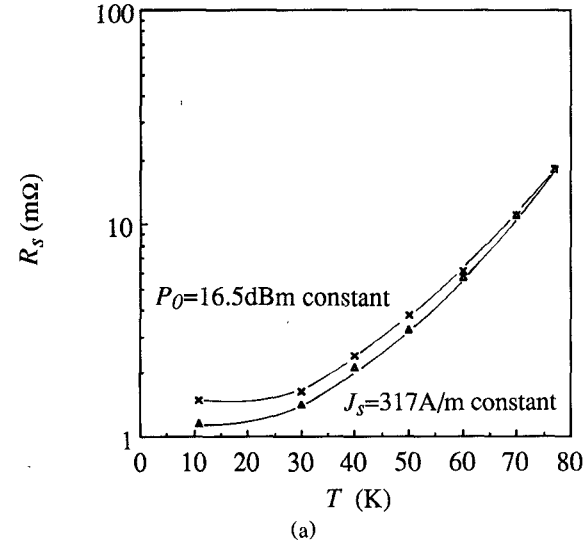

(a)

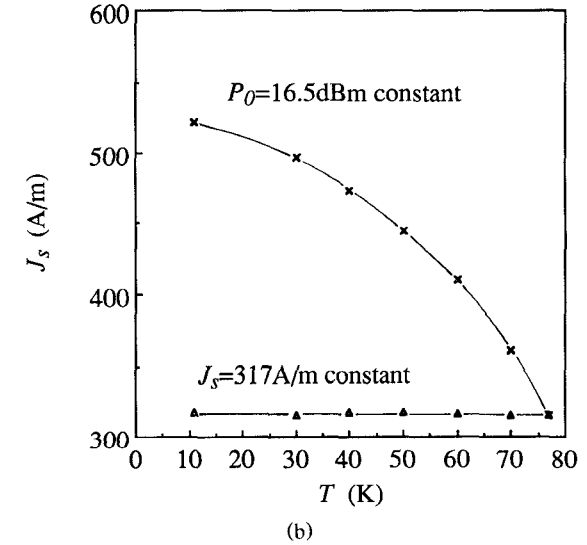

(b)

Fig. 10. Measured results of R_s and J_s versus T when $P_O = 16.5$ dBm constant and when P_O is adjusted to keep $J_s = 317$ A/m constant. (a) R_s versus T. (b) J_s versus T.

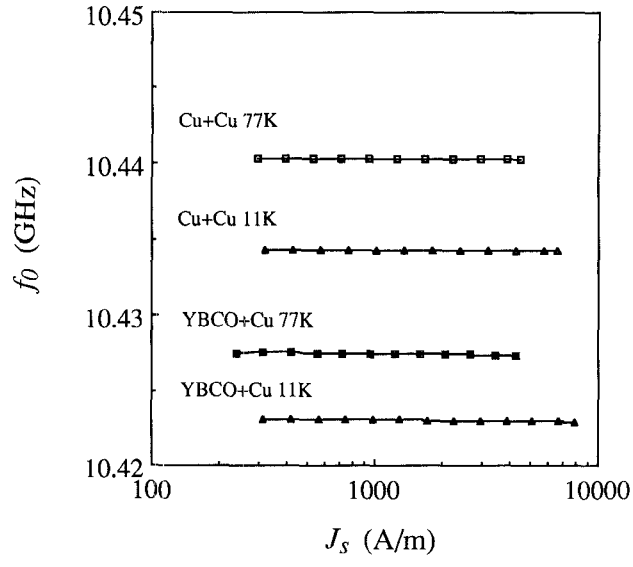

(a)

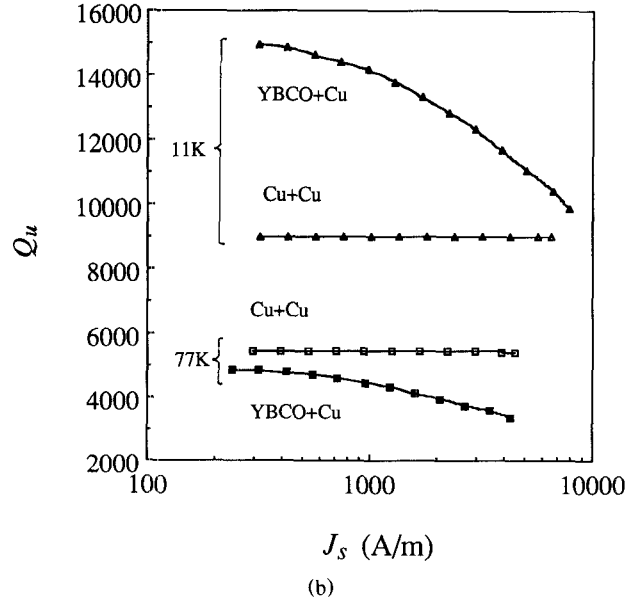

(b)

Fig. 11. J_s dependences of f_0 and Q_u for YBCO by dielectric resonator method. (a) f_0 versus J_s. (b) Q_u versus J_s.

C. J_s Dependence of Z_s for YBCO

For the YBCO and copper plates, the J_s dependences of f_0 and Q_u were measured at 77 and 11 K by using the TE_{011} mode dielectric resonator. These results are shown in parts (a) and (b) of Fig. 11. For the copper both f_0 and Q_u do not depend on J_s. For the YBCO, on the other hand, f_0 decreases about 0.15 MHz with increasing J_s because of the increase of the skin depth; this corresponds to a 3% increase in X_s. Also, the difference between f_0 for the YBCO and that for copper can be attributed to the uncertain contacts described above. Furthermore the J_s dependence of R_s calculated using Fig. 11 is shown in Fig. 12. As a result, R_s of the copper does not depend on J_s, but the value for the YBCO has a strong J_s dependence. When J_s increases from 300 to 7000 A/m, the R_s value of YBCO at 11 K increases more than 400%. Also, the solid triangles in Fig. 12 indicate the

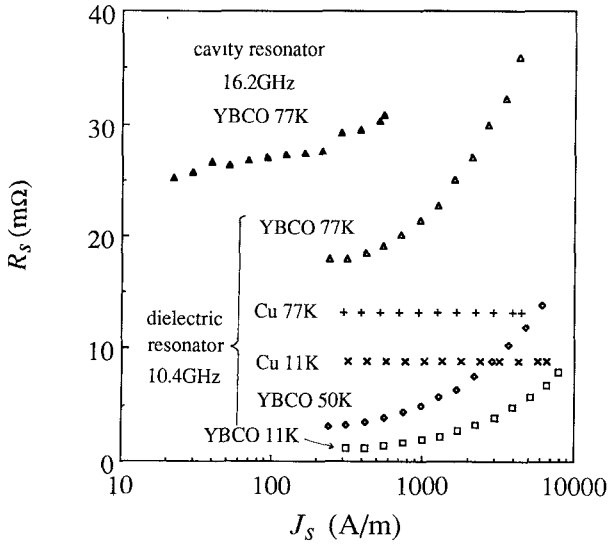

Fig. 12. J_s dependence of R_s for YBCO plate and copper plate.

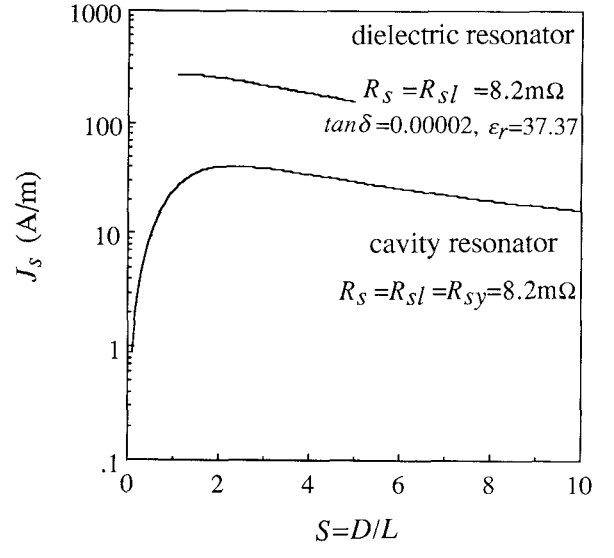

Fig. 13. Calculated values of J_s versus $S = D/L$ for dielectric and cavity resonators when $f_0 = 10.4$ GHz, $P_O = 20$ dBm, and $IL = -30$ dB.

results measured at 16.2 GHz using a cavity resonator with $D = 24.3$ mm and $L = 25.0$ mm. When $P_O = 13$ to 40 dBm (0.02 to 10 W) and $IL = -3$ to -10 dB, the ranges of J_s are from 30 to 700 A/m for the cavity and from 300 to 7000 A/m for the dielectric resonator. A similar result for energy concentration in the dielectric is also obtained from J_s versus $S = D/L$ calculated for the dielectric and cavity resonators when $f_0 = 10.4$ GHz, $P_O = 20$ dBm, and $IL = -30$ dB, as is shown in Fig. 13. As a result, the dielectric resonator method is preferred for measuring the J_s dependence of Z_s because of the energy concentration in dielectric.

IV. Conclusion

Perturbation formulas for a TE_{011} mode dielectric resonator and for a TE_{011} mode cavity resonator have been derived to measure the surface impedance, Z_s, of superconductors. Also, the relationship between the maximum surface current density, J_s, on a superconductor and the output power from a signal generator, P_O, has been derived. On the basis of these analytical results, a measurement technique has been proposed for evaluating the temperature and surface current dependence of Z_s. For a YBCO plate, the temperature dependences of X_s and R_s have been obtained from f_0 and Q_u measured for a TE_{011} mode dielectric resonator. Also, the temperature dependences of δ and λ and σ_r and σ_i have been obtained from these R_s and X_s values on the basis of the two-fluid model. These measured results agree well with the theoretical curves calculated by introducing the concept of the residual normal state conductivity, σ_{res}. This result verifies the validity of this theory for at least one sample of YBCO bulk materials. Furthermore it is verified that a dielectric resonator is preferred for measuring the J_s dependence of Z_s, because of energy concentration.

In addition, this technique is sufficiently sensitive for measuring the R_s of superconducting films in $T < T_c$, although difficulty in measuring X_s is to be expected because the thickness of the films is usually less than the skin depth in normal state ($T > T_c$).

Appendix I
Surface Impedance Z_s

Generally, surface impedance, Z_s, is defined as the ratio of the electric field, E_t, to the magnetic field, H_t, tangential to a conductor surface:

$$Z_s = \frac{E_t}{H_t} = R_s + jX_s = \frac{j\omega\mu}{\gamma} \tag{A1}$$

where γ is the propagation constant in superconductor. In a normal state for $T > T_c$, γ is given by

$$\gamma = \sqrt{j\omega\mu\sigma} = \frac{1}{\delta} + j\frac{1}{\delta} \tag{A2}$$

with

$$\delta = \sqrt{\frac{2}{\omega\mu\sigma}} \qquad \sigma = \frac{\bar{\sigma}\sigma_0}{1+\alpha(T-293)} \tag{A3}$$

where δ is the skin depth, σ is the conductivity, $\sigma_0 = 58 \times 10^6$ S/m for standard copper, $\bar{\sigma}$ is the relative conductivity, and α is the temperature coefficient of resistivity. Substitution of (A2) into (A1) yields

$$Z_s = \sqrt{\frac{\omega\mu}{2\sigma}} + j\sqrt{\frac{\omega\mu}{2\sigma}}\,. \tag{A4}$$

In a superconducting state for $T < T_c$, on the other hand, γ is given by

$$\gamma = \sqrt{j\omega\mu\sigma_s} = \sqrt{\frac{1}{\lambda^2} + j\frac{2}{\delta^2}} \tag{A5}$$

according to the two-fluid model [1], where σ_s is the complex superconducting state conductivity, and λ is the penetration depth at T K. In this case, substitution of

(A5) into (A1) yields

$$R_s = \frac{\omega\mu\lambda}{\sqrt{2}}\sqrt{\frac{\sqrt{1+4(\lambda/\delta)^4}-1}{1+4(\lambda/\delta)^4}} \tag{A6}$$

$$\approx \frac{\mu^2\sigma\lambda^3}{2}\omega^2 \qquad (\lambda \ll \delta) \tag{A7}$$

$$X_s = \frac{\omega\mu\lambda}{\sqrt{2}}\sqrt{\frac{\sqrt{1+4(\lambda/\delta)^4}+1}{1+4(\lambda/\delta)^4}} \tag{A8}$$

$$\approx \mu\lambda\omega \qquad (\lambda \ll \delta). \tag{A9}$$

From (A6) and (A8), we also obtain

$$\delta = \frac{R_s^2 + X_s^2}{\omega\mu\sqrt{R_s X_s}} \qquad \lambda = \frac{R_s^2 + X_s^2}{\omega\mu\sqrt{X_s^2 - R_s^2}}. \tag{A10}$$

Furthermore, σ_s is derived from (A5); that is,

$$\sigma_s = \sigma_r - j\sigma_i = \frac{2}{\omega\mu\delta^2} - j\frac{1}{\omega\mu\lambda^2}. \tag{A11}$$

In this paper the relation $\sigma_r = \sigma_n(T/T_c)^4 + \sigma_{\text{res}}$ is introduced, where σ_n is the normal state conductivity and σ_{res} is the residual one determined from the measured value of σ_r.

Appendix II
The Derivation of (3)

The characteristic equation for a TE_{01l} mode dielectric rod resonator as shown in Fig. 1(a) is given by

$$u\frac{J_0(u)}{J_1(u)} = -v\frac{K_0(v)}{K_1(v)} \tag{A12}$$

where

$$u = k_{r1}R = R\sqrt{\epsilon_r k^2 - \beta^2} \tag{A13}$$

$$v = k_{r2}R = R\sqrt{\beta^2 - k^2} \tag{A14}$$

$$u^2 + v^2 = (\epsilon_r - 1)(kR)^2 \tag{A15}$$

$$k = \frac{\omega}{c} \qquad \beta = \frac{l\pi}{L} \tag{A16}$$

and $K_n(v)$ is the modified Bessel function of the second kind.

When $l = 1$, we shall derive (3) below using (A12)–(A16). From (1) and (A1), we first obtain the following relation:

$$\frac{1}{\gamma} = \frac{L'\cot X}{X} \tag{A17}$$

where

$$X = \beta L\left\{1 - \frac{\pi}{2\beta L}\right\} = \beta L' \tag{A18}$$

$$L' = L\left\{1 - \frac{\pi}{2\beta L}\right\}. \tag{A19}$$

When the superconductor plate has loss, $\delta \neq 0$; so X changes to $X + \Delta X$. Therefore, $1/\gamma$ is given by

$$\frac{1}{\gamma} = \frac{L'\cot(X+\Delta X)}{X+\Delta X} \approx -L\frac{\Delta\beta}{\beta}. \tag{A20}$$

Then the total differentiations of (A14) and (A15) yield

$$\frac{\Delta v}{v} = \left(\frac{R}{v}\right)^2\left\{\beta^2\frac{\Delta\beta}{\beta} - \left(\frac{\omega}{c}\right)^2\frac{\Delta\dot{\omega}}{\omega}\right\} \tag{A21}$$

$$\frac{\Delta v}{v} = \frac{\epsilon_r - 1}{1+W}\left(\frac{R}{v}\right)^2 k^2\frac{\Delta\dot{\omega}}{\omega} \tag{A22}$$

respectively, where

$$\frac{du^2}{dv^2} = \frac{u\,du}{v\,dv} = W. \tag{A23}$$

From (A20)–(A22), we obtain

$$\frac{1}{\gamma} = -L\left(\frac{k}{\beta}\right)^2\frac{\epsilon_r + W}{1+W}\frac{\Delta\dot{\omega}}{\omega}. \tag{A24}$$

Furthermore, substitution of (A24) into (A1) gives (3).

Appendix III
The Derivation of P_d, P_u, and P_l

For a TE_{01l} mode dielectric rod resonator, the values of P_d, P_u, and P_l are calculated from the following relations:

$$P_d = \omega\tan\delta\left\{\frac{\epsilon_0\epsilon_r}{2}\int_0^R\int_0^{2\pi}\int_0^L |E_{\theta 1}|^2 r\,dr\,d\theta\,dz\right\} \tag{A25}$$

$$P_u = \frac{R_s}{2}\left\{\int_0^R\int_0^{2\pi}|H_{r1(z=L)}|^2 r\,dr\,d\theta + \int_R^\infty\int_0^{2\pi}|H_{r2(z=L)}|^2 r\,dr\,d\theta\right\} \tag{A26}$$

$$P_l = \frac{R_{sl}}{2}\left\{\int_0^R\int_0^{2\pi}|H_{r1(z=0)}|^2 r\,dr\,d\theta + \int_R^\infty\int_0^{2\pi}|H_{r2(z=0)}|^2 r\,dr\,d\theta\right\} \tag{A27}$$

where the field components are given by

$$H_{z1} = -A(k_{r1}/\beta)J_0(k_{r1}r)\sin\beta z \tag{A28}$$

$$H_{r1} = AJ_1(k_{r1}r)\cos\beta z \tag{A29}$$

$$E_{\theta 1} = A(j\omega\mu_0/\beta)J_1(k_{r1}r)\sin\beta z \tag{A30}$$

inside the rod and by

$$H_{z2} = B(k_{r2}/\beta)K_0(k_{r2}r)\sin\beta z \tag{A31}$$

$$H_{r2} = BK_1(k_{r2}r)\cos\beta z \tag{A32}$$

$$E_{\theta 2} = B(j\omega\mu_0/\beta)K_1(k_{r2}r)\sin\beta z \tag{A33}$$

outside the rod with

$$\frac{B}{A} = -\frac{uJ_0(u)}{vK_0(v)} = \frac{J_1(u)}{K_1(v)}. \tag{A34}$$

ACKNOWLEDGMENT

The authors would like to thank M. Katoh for fabrication of the resonators and R. Kitaichi and C. Chu for their assistance with the experiment.

REFERENCES

[1] W. H. Hartwig, "Superconducting resonators and devices," *Proc. IEEE*, vol. 61, pp. 58–70, Jan. 1973.
[2] J. R. Delayen and C. L. Bohn, "Temperature, frequency, and rf field dependence of the surface resistance of polycrystalline $YBa_2Cu_3O_{7-x}$," *Phys. Rev. B*, vol. 40, 7, pp. 5151–5154, Sept. 1989.
[3] S. J. Fiedziuszko and P. D. Heidmann, "Dielectric resonator used as a probe for high T_c superconductor measurements," in *IEEE MTT-S Int. Microwave Symp. Dig.*, June 1989, pp. 555–558.
[4] D. E. Oates, A. C. Anderson, and B. S. Shih, "Superconducting stripline resonators and high-T_c materials," in *IEEE MTT-S Int. Microwave Symp. Dig.*, June 1989, pp. 627–630.
[5] K. Aida and T. Ono, "Microwave surface resistance measurement technique for cylindrical high-T_c superconductor," in *IEEE MTT-S Int. Microwave Symp. Dig.*, June 1989, pp. 559–562.
[6] A. Fathy *et al.*, "Microwave properties and modeling of high-T_c superconducting thin film meander line," in *IEEE MTT-S Int. Microwave Symp. Dig.*, May 1990, pp. 859–862.
[7] R. Dill *et al.*, "Testchip for high temperature superconductor passive devices," in *IEEE MTT-S. Int. Microwave Symp.*, May 1990, pp. 863–866.
[8] R. B. Hammond *et al.*, "Superconducting Tl-Ca-Ba-Cu-O thin film microstrip resonator and its power handling performance at 77 K," in *IEEE MTT-S Int. Microwave Symp. Dig.*, May 1990, pp. 867–870.
[9] Y. Kobayashi, T. Imai, and H. Kayano, "Microwave measurement of surface impedance of high-T_c superconductor," in *IEEE MTT-S Int. Microwave Symp. Dig.*, May 1990, pp. 281–284.
[10] Y. Kobayashi, T. Imai, and H. Kayano, "Microwave measurement of current dependence of surface resistance for high-T_c superconductor," in *Proc. 3rd Asia-Pacific Microwave Conf.*, Sept. 1990, pp. 489–492.
[11] Y. Kobayashi and M. Katoh, "Microwave measurement of dielectric properties of low-loss materials by the dielectric rod resonator method," *IEEE Trans. Microwave Theory Tech.*, vol. MTT-33, pp. 586–592, July 1985.
[12] Y. Kobayashi and T. Imai, "Phenomenological description of conduction mechanism of high-T_c superconductors by three-fluid model," *IEICE Trans. Commun.*, vol. E74, July 1991 (in press).

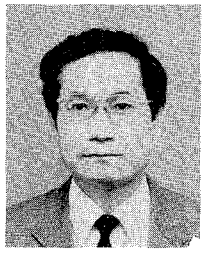

Yoshio Kobayashi (M'74) was born on July 4, 1939. He received the B.E., M.E., and D.Eng. degrees in electrical engineering from Tokyo Metropolitan University, Tokyo, Japan, in 1963, 1965, and 1982, respectively.

He was a research Assistant from 1965 to 1968, a Lecturer from 1968 to 1982, and an Associate Professor from 1982 to 1988 in the Department of Electrical Engineering, Saitama University, Urawa, Saitama, Japan. He is now a Professor there. His current research interests are in dielectric resonators, dielectric filters, measurement of dielectric materials, and properties of high-T_c superconductors in the microwave and millimeter-wave regions.

Dr. Kobayshi is a member of the IEE of Japan.

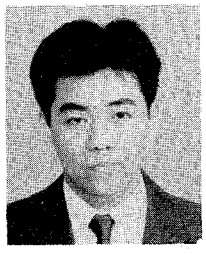

Tadashi Imai was born in Saitama, Japan, on August 18, 1965. He received the B.E. and M.E. degrees in electrical engineering from Saitama University in 1989 and 1991 respectively. His research as a student focused on the microwave properties of high-T_c superconductors.

In April 1991, he joined Canon Electronics Inc., Chichibu, Saitama, Japan.

Mr. Imai is an associate member of the Institute of Electronics, Information and Communication Engineers of Japan.

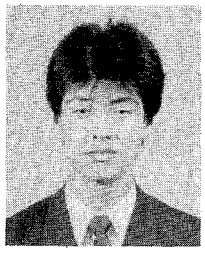

Hiroyuki Kayano was born in Saitama, Japan, on July 16, 1967. He received the B.E. degree in electrical engineering from Saitama University, Saitama, Japan, in 1990. Currently, he is studying toward the M.E. degree at the same university. His research activities have dealt with the microwave properties of high-T_c superconductors.

Mr. Kayano is an associate member of the Institute of Electronics, Information and Communication Engineers of Japan.